

《解説》

Capillarity Phenomena and Metal-Dielectric Interaction in Zeolite Channels

Valentin N. Bogomolov

Ioffe Phys. Tech. Inst., St. Petersburg, Russia

A simple model of transition metal-dielectric layer based on the experimental data on the capillary phenomena for the 6/12 Å diameter channels and on the Van der Waals bond as a weak excimer interaction of the fluctuation nature is considered. Some aspects of interphase interaction for adsorption, catalysis, energetics, and electronics problems were discussed.

Intermediate layers between the different phases are very widespread and important objects for heterogeneous systems equilibrium, chemical reactions velocity, catalysis, micro- and nano-electronic devices and so on. The microscopic structure of the extremely thin transition layers and the local interactions are very difficult for the experimental investigations.^{1, 2, 3)} The most direct and adequate method of investigations of this problem is examination of capillary phenomena in the atomic diameter channels. Such experiments were undertaken as an attempts to create the low-dimensional systems by means of the matrix method. It was a task in line with the HTSC- problem. The rutile (TiO₂) monocrystals with a 4-member spiral structure channels as a matrix were utilized for that purpose and the zeolites monocrystals with the 6/12 Å diameter channels were the next.⁴⁾

The simplest model for the two phases contact is the some surface without the thickness and with surface tension σ . When the interphase boundary become curved the pressure difference P between the phases may be expressed via the surface tension σ and the curvature radius r by means of the Laplace equation $P=2\sigma/r$.¹⁾ Apparently Poisson was the first who understand that the capillary phenomena were consequences of the finite thickness of the capillary layer. Along the intermediate layer properties of the both phases must altered relatively fluently. As with

most research, this concept has raised a new problems of the properties of this layer which may be considered as a new physical object. For example the surface tension of the spherical drop (one phase situation, vapor pressure absent) depend on the surface curvature radius r :

$$\begin{aligned}\sigma_s(r)/\sigma_o &\simeq r_s^2/(r_s + \delta_{po})^2 \simeq 1 - 2\delta_{po}/r_s; \\ \sigma_s(r) &\simeq \sigma_o - \delta_{po}P,\end{aligned}$$

where P is the Laplace pressure, $\sigma_o = \sigma(\infty)$, $\delta_{po}P$ is the elastic energy of the interphase layer volume. In that case the surface of tension (r_s) is not coincide with the equimolar surface (r_e) (see Fig. 1a). Tolman length δ_{po} is the difference between these surface curvature radii $r_e - r_s$ and it determines the surface tension versus the pressure dependence. It depend on the compressibility k of the volume and on the surface and volume properties difference.

The simplest case of the two phase interaction is the liquid-metal-dielectric contact. This type of interaction is of importance for adsorption and catalysis, for capillary and electrocapillary energetics, for composites and electronic devices, and other.⁶⁾ It becomes possible to directly determine the properties of the interphase layer and the dependence of the surface energy on the curvature when channels of single-crystal zeolite are employed. Fortunately, the channel diameters are known with crystallographic precision (6.7 × 7.0 Å in

mordenite and 11.7 Å in zeolite X) and the channels have a high degree of monodispersion and a high density (the channel volume is as much as 50% of the volume of the X-crystal).⁵⁾ The capillary walls in zeolites consists of the oxides Al₂O₃ and SiO₂ with saturated valence and have no broken bonds (“molecular” surface) in contrast to the surface created by mechanical methods. However in such capillaries there are two types of interphase boundaries present simultaneously: liquid-vapor and liquid-solid insulator, along with four kinds of curvature: spherical and cylindrical, positive and negative (for window regions between the zeolite cavities).

Experimental investigations of the capillary phenomena in zeolite channels give an information on the liquid metal-dielectric interaction and one may introduce a qualitative description of the some phenomena observed. So an interphase gap $h \approx (1.1/1.5)$ Å between the liquid metal and dielectric wall with the compressibility $\kappa \approx 4 \cdot 10^{-5} \text{ atm}^{-1}$ was observed and the interphase metal-dielectric interaction energy as a function of the metal surface tension and of the Laplace pressure was measured.^{4,6)} It was shown that the well known picture of the capillary phenomena remains for the atomic diameter channels also.

Thermodynamic theory of capillarity does not depend on the nature of the interacting phases but at the some time it can not answer the question on the local structure of interphase interaction and its microparameters, on the magnitude and sign of the Tolman length.^{1,2)} Thorough understanding of the problem must involve the physical approach also. The simplest example of the problem is determination of the magnitude and sign of the Tolman length for metallic drop in vacuum at $T=0$. The above mentioned well-known Gibbs-Tolman-Koenig-Buff (GTKB) formula describes the dependence of surface tension on the diameter of a free spherical drop. The GTKB equation also describes the dependence of surface energy on the interphase pressure or Laplace pressure when the second phase is vacuum. For metals the vapor pressure at

moderate temperatures is small. For $\delta_{po}/r=1$ the approximate GTKB formula differs from the exact formula by 10%.¹⁾ The length $\delta_{po} = -d\sigma/dP$. If Tolman length δ_{po} negative, the surface tension increases as the drop diameter decreases (as the Laplace pressure increases) and vice versa.

The magnitude and sign of δ_{po} can be evaluated from very simple considerations. The change in the interatomic distance “ a ” associated with compression or heating, must cause a change $\sigma \sim a^{-n}$. After a simple transformations one can obtain

$$\begin{aligned} d\sigma/dP &= n\sigma\kappa/3; \quad d\sigma/dT = -n\sigma\beta/3; \\ d\sigma/dP &= -(\kappa/\beta)d\sigma/dT \end{aligned}$$

where κ is the compressibility, β is the volume thermal expansion coefficient, $d\sigma/dT$ is the entropy of the surface. These quantities are well-known from the experimental data in contrast to the Tolman length. For majority of metals at the melting temperatures we have $d\sigma/dT \approx -(0.1/0.3) \text{ erg/cm}^2 \text{ deg}$, that corresponds approximately to $n \approx 6$. This yields $d\sigma/dP \approx 2\kappa\sigma$. Hence for K and Na we have $\delta_{po} \approx -0.7$ Å, while for the other metals $\delta_{po} \approx -(0.2/0.3)$ Å. It is not surprising since the $d\sigma/dP = -(d\sigma/dT)/rc_v$, where r is the Gruneisen constant and c_v is the volumetric specific heat. The sign of the effect in this case correspond to σ increasing as the diameter decreases (as the pressure increases) in agreement with the calculated results.²⁾ Evaluation of the Tolman length if $2r \approx a$ may be made also from the well-known atomic Goldschmidt contraction for metals. When the number N of the nearest neighbour atoms is lowered from 12 to 0, the atom diameter decrease: $d_N/d_{12} \rightarrow \sim 0.8$; $(d_{12}^3 - d_0^3)/d_{12}^3 \approx k4\sigma(d_0)/d_0$. It is easy to show that

$$\begin{aligned} 1 &\geq d_0/d_{12} \\ &= \{ [1 + (1 - |\delta_{po}|8/d_{12})^{1/2}] / 2 \}^{1/3} \geq 0.79 \end{aligned}$$

That way also gives for δ_{po} value in the order of magnitude obtained above: $|\delta_{po}| < d_{12}/8$. Pure thermodynamic considerations let us make the conclusion on the some interphase transitional layer existence. But the question

about the layer nature is opened. If one accept the supposition that δ_{po} exist in reality and in first approximation does not depend on the curvature radius r , it must be mentioned that the space scale for this layer corresponds only to that of atomic orbital splitting.⁷⁾ Out of the metal volume the excited state orbitals of various nature are situated. For very small metal clusters the atom-like model of electron energy is valid and the excited state orbitals are the cluster orbitals. Variation in energy of the cluster by some perturbation induces the corresponding variation in cluster diameter the latter is determined as a position of the principal maxima in electron radial distribution function.⁷⁾ From the other hand a substance composed by the atoms in excited state (excimer state) must have the volume greater than that of the substance in ground state. These considerations are valid for the surface also. In order to display the existence of the interphase layer it is necessary to induce the occupation of the cluster or surface excited state orbitals by means of some perturbation. Part of electrons displaces from the atoms on the surface out of the volume. That may lead to lowering of the local density of states of the surface atoms also. Such effect have been observed in experiment.⁸⁾ This picture is not in contradiction with the thermodynamic scheme (Fig. 1 b).

When the zeolite channels are filled with the liquid metal one has a three-dimensional liquid metal "sublattice" with the well defined surface of metal (0.2/0.5 Å accuracy). This surface may serve as a sound probe for the dielectric surface investigation.

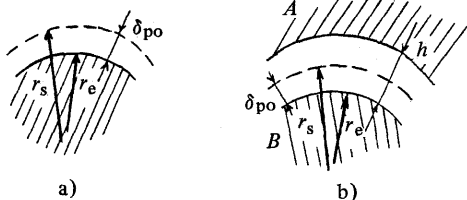


Fig. 1 a) Metal-vacuum boundary thermodynamic scheme,
b) Interphase layer thermodynamic scheme.

A weak metal-dielectric interaction is displayed in wetting (Adhesion energy σ_c). One can define the surface energies as follow: σ_t for solid surface, σ_o for liquid surface, σ_{to} for interphase layer. The contact angle α , Laplace pressure P_k , surface and adhesion energies are connected with the help of the Young, Dupre and Laplace equations (Fig. 2, inset):

$$\begin{aligned}\sigma_t &= \sigma_{to} - \sigma_o \cos \alpha; \sigma_c = \sigma_o + \sigma_t - \sigma_{to}; \\ \sigma_k &= \sigma_o - \sigma_c = \sigma_o \cos \alpha = P_k r/2\end{aligned}$$

Total surface energy exceeds the free surface energy (surface tension) by the entropy item $Td\sigma/dT$. The last contribution is small when the temperature is low relatively to the critical temperature.

Using the Berthelot relation for interaction constants of molecules O and T: $C_{OT} = (C_{OO}C_{TT})^{1/2}$, Girifalco and Good (GG) have obtained a simple expression for van der Waals (VDW) interaction energy between the two phases⁹⁾:

$$\begin{aligned}\sigma_c &= 2M(\sigma_o\sigma_t)^{1/2} = \sigma_o + \sigma_t - \sigma_{to}; \\ M &= 4r_o r_t / (r_o + r_t)^2\end{aligned}$$

where $r_{o,t}$ are the mean radii of the particles in the different phases.

Earlier Pauling has utilized this relation for the electronegativity scale determination in the case of the covalent bonds.¹⁰⁾

Surface energy σ_t of the solid body one can find by means of the contact angle measurements and with the help of the GG formula.

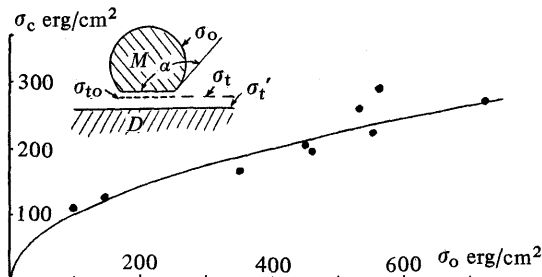


Fig. 2 Metal-zeolite adhesion energy σ_c on the metal surface energy σ_o dependence (points). Solid line corresponds $\sigma_c = 2(\sigma_{to} \sigma_o)^{1/2}$ at $\sigma_t = 25$ erg/cm². Inset — metal drop on the dielectric surface.

Series of such experiments were performed for the mercury and the dielectrics with the different chemical nature contact.⁹⁾ Values from several — units up to several tens erg/cm² were calculated for different materials. Another case — using of the different liquid metals with the surface tension σ_o (100/700 erg/cm²) and one and the some dielectric (zeolite) in contact for precise determination of σ_t of the dielectric.⁶⁾ The points in Fig. 2 indicate the values of adhesion energy σ_c obtained by calculations with the help of the above mentioned relations and experimental data on σ_k .⁶⁾ Adhesion energy has a two parts $\sigma_c(\sigma_o; P_k) = \sigma_{co}(\sigma_o; 0) + \delta_c P_k(\sigma_o)/2$, where $\sigma_{co}(\sigma_o; 0)$ is the initial adhesion energy at the interphase pressure $P_k=0$. A Tolman length $\delta_c \approx (1.2/1.5) \text{ \AA}$ is a proportional coefficient between the interphase (Laplace) pressure and the additional adhesion energy. The Tolman length δ_c was determined only in order of magnitude so far as $\sigma_{co} \approx 110 \text{ erg/cm}^2$ as a constant and independent on σ_o was used.⁶⁾

For the zeolite case one has a dielectric surface with no broken bonds and no Tamm-levels (quasimolecular surface). But it does not mean that surface energy σ_t' is absent (inset in Fig. 2). Own surface energy σ_t' for zeolites is about 900 erg/cm² according to the calorimetric data and to the evaluations with the help of the GG formula and the water adsorption energy $\sigma_{co} \approx 300 \text{ erg/cm}^2$. Berthelot relation is also valid for wetting contact.

Zeolite monocrystals are the metastable systems. Their chemical bond energy is smaller than that of the Al₂O₃ and SiO₂ bulk materials. Part of the chemical valence bond energy is spread over the channels surface and this energy display itself as an ability for VDW interaction. It is the base for the zeolites utilization as a powerful tool for chemical technology. There are many examples of the transition of the chemical bond energy into the different forms. For example the mechanochemical activation process may be mentioned. Surface energy σ_t' of the zeolite channels is about 0.6 kcal/g. Energy capacity of such order of magnitude is ordinary for

explosive substances like trotyl. There is a possibility of the explosive substances fabrication if to use zeolites.

The solid line in Fig. 2 corresponds to GG formula $\sigma_c = 2(\sigma_c \sigma_t)^{1/2}$, when $\sigma_t = 25 \text{ erg/cm}^2$. Solid surface energy σ_t in order of that obtained in.⁹⁾ Thus there is the essential difference between the effective surface energy $\sigma_t = 25 \text{ erg/cm}^2$ of the solid dielectric and own surface energy $\sigma_t' = 900 \text{ erg/cm}^2$ if the contact metal-dielectric is present. Such discrepancy has been observed earlier.¹¹⁾ It must be taken into account the fact that the wetting liquids fill the channels completely, while a liquid metals fill only a part of the channel volume. A gap $h = (1.1/1.5) \text{ \AA}$ exists between the wall of the zeolite channel and the liquid metal surface. The magnitude of this gap is near the interphase Tolman length.⁶⁾ Qualitatively the difference between the two kinds of the surface energy for zeolite one can understand from the following consideration. Orbital radii of the excited states for atoms on the surface are greater than radii of the ground state. Above the surface of the dielectric a planar network of the electronic excited states at the distance $\sim h$ appears under the influence of the metal-dielectric perturbation interaction (Fig. 3a). Because of the fluctuation nature of the interaction mean occupancy of the excited states $X < 1$. The case $X = 1$ correspond to an excimer state. Appearing of the excited states with $X < 1$ above the dielectric surface prevents the direct contact of the metal surface with the dielectric high energy surface from one side and rises the VDW interaction energy σ_c from the other.

Typical example of the VDW materials is the condensed inert gases (IG). VDW radii of the IG atoms are close to that of the atom excited state orbitals and to the atomic radii of corresponding alkaline metals. Density of the condensed IG is close to that of the corresponding alkaline metals. In the case of the IG atoms the bond can be treated approximately as though it were metallic type bond, but resulting from the orbitals of an excited state whose mean occupation $X < 1$ (life time

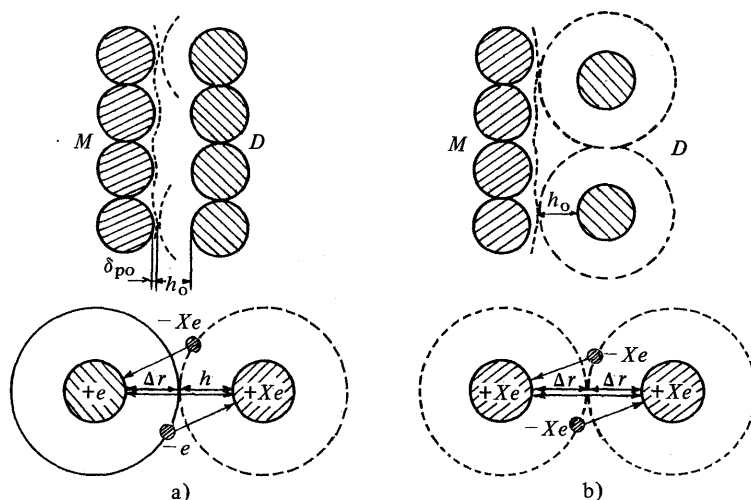


Fig. 3 a) Metal-dielectric boundary and metal-dielectric interaction schematic picture.
b) Metal-VDW condensate boundary and dielectric-dielectric interaction schematic picture.

about 10^{-10} sec.). Under the high pressure the condensed IG become metals ($X \approx 1$) with inter-atomic distances sufficiently greater than the diameters of the ground state orbitals.

Transition of the atoms from the ground state into excited state depend on the relation between the transition energy ΔE and the mean perturbation energy ε . If the perturbation energy has a fluctuation nature the occupation X may be expressed by means of the factor $\exp(-\Delta E/\varepsilon)$, similar to the Boltzmann factor. Now the liquid IG can be regarded as weak excimer analog of an alkaline metal (occupation of the excited states $X < 1$). Since for simple metals the bond energy $\sim e^2/r_m$, for the liquid IG one can write $q_{VDW} = C_1 e^2 X^2 / r_{VDW}$. The occupation X depends on the difference between the energies of the excited and ground states ΔE and on the magnitude of the Coulomb perturbations interaction ε of the atomic shells by one another $X \approx \exp(-\Delta E/\varepsilon)$, where $\varepsilon = A e^2 / 2 \Delta r + B e^2 X / \Delta r = e^2 (A + 2BX) / 2 \Delta r = e^2 Z / 2 \Delta r$ (see Fig. 3b). Δr is the radii difference of the excited and ground state. Surface energy and binding (condensation) energy are connected.¹¹⁾ Therefore surface energy of the liquid IG is $\sigma_{VDW} \approx C_2 e^2 X^2 / r_{VDW}$.

A simple model of VDW bond as a weak excimer interaction may be easily employed for the metal-dielectric adhesion energy calculation. At a metal-dielectric contact the filled orbitals of the metal interact with the partly filled orbitals of the excited state of the dielectric surface (see Fig. 3a):

$$\begin{aligned} \sigma_{co} &= C_3(-e)(eX) + C_4(e)(-eX) = 2C_5 e^2 X \\ &= 2(C_6 e^2 C_7 e^2 X^2)^{1/2} = 2C_8 (\sigma_o \sigma_{VDW})^{1/2} \\ &= 2C_8 (\sigma_o \sigma_t)^{1/2} \end{aligned}$$

Therefore the excimer model of VDW metal-dielectric interaction is satisfied the Berthelot relation if the solid state surface energy of dielectric corresponds to that of the some equivalent VDW condensate. Surface energy $\sigma_t = 25$ erg/cm² of the partially filled excited states at the dielectric surface is corresponded to the surface energy of Kr. Kr atoms has $\Delta r \approx 1.3$ Å, $\Delta E = 10$ eV. Energy of such magnitude may affect on the metal-dielectric contact parameters only. This is in accordance with the results of introducing mercury into zeolite X at 20°C and at 400°C. Any difference in the contact angle (Laplace pressure) except the case of the $d\sigma/dT$ - dependence was not observed.

If we use above mentioned capillary re-

lations together with the GG formula, then we can obtain an expression for the interphase energy σ_{to} : $(\sigma_{to})^{1/2} = (\sigma_o)^{1/2} - (\sigma_t)^{1/2}$. It means that the interphase surface energy is the result of the difference between the electron concentrations in the vicinity of the metal surface and on the excited state surface of dielectric:

$$X_{to} = X_o - X_t; (X_o \approx 1).$$

If the interphase energy $\sigma_{to} = \sigma_o + \sigma_t - \sigma_c$, we can define the interphase Tolman length as $\delta_{to} = \delta_{po} + \delta_t - \delta_c$. A simple calculations give:

$$\begin{aligned} \delta_c &= -d\sigma_c/dp \approx -[1 + F(\Delta E; h)] \sigma_c k_h \\ &\approx -(1/1.5) \text{ \AA}; \delta_{to} > 0 \end{aligned}$$

for the experimental value $k \approx 4 \cdot 10^{-5} \text{ atm}^{-1}$ and if $\Delta E \approx 10 \text{ eV}; \delta_t < \delta_{to}$.

The picture of the metal-dielectric interphase layer described above is in agreement with that obtained by the thermodynamic approach (Fig. 1b). If the gap $h_o = h - \delta_{po}$ can be treated approximately as though it was interphase Tolman length it is greater than the Tolman length of metal and has an opposite sign. It means that as the interphase pressure increases, the interphase surface energy falls of due to the rise in adhesion (wetting) energy. At the high pressure (or small radii) the energetic boundary between the phases may disappear. Excimer model of the metal-dielectric contact is not in contradiction with the realistic parameters of the system.

Now we shall regard the VDW bond as a quasi-chemical metal-type interaction by means of the partially filled orbitals of the excited state in contrast to chemical bond as an interaction of the ground state orbitals.

One can make some another conclusions about the metal-dielectric and dielectric-dielectric contacts from this point of view.

There are some instability in X magnitude if the X -dependent members in the Coulomb perturbation energy were taken into account. Instability in system of the excited states occurs at the certain relation between the parameters. Equation:

$$(A + 2BX) \ln X = -2\Delta E \Delta r / e^2 = -r$$

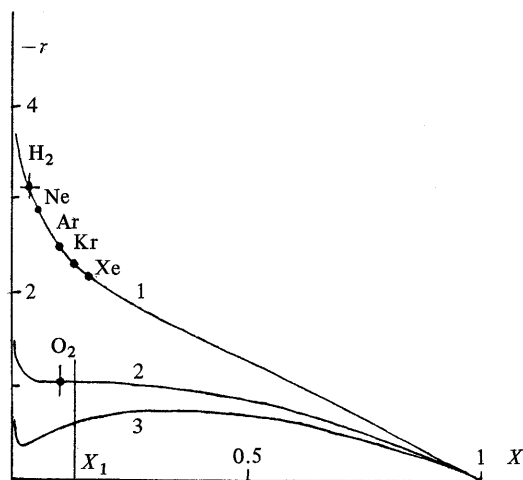


Fig. 4 $Z(X) \ln X = -r$ dependence at $B = 1, A = 1.09$ (1); $A = 1/3.6$ (2); $A = 1/20$ (3). X_1 : extremum position.

has a graph shown in Fig. 4. Numerical evaluations of the condensation energy of the IG, H_2, N_2, CO with the help of the excimer formulae are close to the experimental data if $A \approx B \approx 1$. The instability point corresponds to $B = 1, A = 2/e^2 = 1/3.7$. Correct condensation energy for O_2 one can calculate only if $A \approx 1/3.6$. In contrast to the rest gases O_2 has a magnetic properties as well as nitrogen oxides and sulphur in molecular forms. These elements are often present in compounds with the phase transition.

It must be emphasize that the model discussed above provides only a simple and qualitative description of the experimental findings.

If the dielectric is in contact with the metal surface, $Z(X)$ must be modified and it may be the reason for the transition of the physical adsorption into the chemisorption and oxygen chemical activity.

For the case of metal-VDW dielectric contact (adsorption layer on the metal surface) electron occupation X of the first layer depends on the Coulomb perturbation:

$$\epsilon_1 = A_1 e^2 / (\Delta r + h) + B_{11} e^2 / h + B_{12} e^2 X_1 / h$$

For the second layer $X_1 > X_2$ so far as $\epsilon_1 > \epsilon_2 = A_2 e^2 / 2h + B_2 e^2 X_2^2 / h$ and so on. Calculated adsorption energy for the Kr and O_2 on the metal surface are shown in Fig. 5. The bond



Fig. 5 Calculated adsorption energy for Kr (1) and O₂ (2) layers at the metal surface.

energy (or adsorption energy) ladder will correspond to the excimer state ladder. These are four distinct steps for Kr case in agreement with the four steps of experimental adsorption isotherm.¹²⁾ The amount of steps depend on the substance parameters. For example there are six clear steps for oxygen adsorption energy along the layer numbers. This picture is in accordance with the calculated “terraced wetting”.¹³⁾ In the model discussed a simple mechanism of the some excitations or the interactions translation on a long distances by means a relay race from atom to atom appears. So, the real transition region between the phases may spread over the several atom layers for the weak bond substances. For the high bond energy substances (zeolites and metals) excitations decrease more rapidly. For example for the platinum cluster the local density of states at the Fermi energy run up to the bulk value at the third layer and depend on the second phase presence.⁸⁾

Metal-dielectric interaction has a direct relation to the catalysis. It is the problem of the chemical reactions between the different adsorbed atoms on the metal surface. So for atoms A and B on the metal surface one may obtain their interaction energy $q_{AB} \sim$

$e^2 X_{Am} X_{Bm} / r_{VDW}$, i.e., the interaction between the atoms A and B on the metallic surface is increased in accordance with the ratio $X_{Am} X_{Bm} / X_A X_B > 1$. Thus on the catalyst surface the catalytic reactor with the high component concentration, high temperature, long time of interaction, and high effective pressure is realized. This mechanism may be of importance for catalytic reactions with the adsorption processes.¹⁵⁾

According to Fig. 2, adhesion energy for metal clusters and dielectric carriers may be of the order of the bond energy for metals, i.e., relatively strong. If the free electrons are appeared in carrier the cluster-carrier interaction may become stronger. Part of the cluster effective valence spends on the cluster-carrier interaction. It displays itself in lowering of the adsorption ability of the clusters. This phenomena may be the cause of the suppression of the gas adsorption after a high-temperature reduction of the metal support system (Pt/TiO₂) in H₂ (catalyst strong metal-support interaction state—SMSI effect).¹⁴⁾

Systems consisting of a liquid and a capillary absorber (hydrocapillary working medium) are of interest, e.g., for several energy-storage devices. When a nonwetting liquid is introduced into a capillary the expended energy is accumulated in the form of the energy of broken chemical bonds of the newly formed surface. It can be recovered as mechanical work when the liquid comes out under pressure (a hydrocapillary or mechanochemical energy store). For $d \approx a$ the energy capacity of such storage device approach that of electrochemical batteries, approximately 200 kJ/l. The advantage of a hydrocapillary storage devices include high power (up to 20 kW/l), constant pressure, total and rapid charging and discharging, the absence of any electric motors and generators, as well as the obvious and immediate possibility of converting them into hydrocapillary machines utilizing the well-known dependence of the surface tension on temperature or on the interphase potential difference (electrocapillary phenomena).

Electrocapillapy phenomena have been

thoroughly studied in the case of contacts between metals and liquid electrolytes having ionic conductivity. The decrease in σ under the influence of the potential difference E results from a buildup of charge q in a double layer and is proportional to the energy of the charges in the interphase capacitor, $\sigma_E = \sigma_0 - CE^2/2$ (an analog of the reduced GTKB-equation). The value of the capacity is $C \approx 30$ mF/cm² and the experimental values of the interface thickness are about 1.5 Å. The interphase tension is several fold for $E \approx 1/5$ V. If we use a conducting matrix with a porosity close to that of zeolite X, the capacitance of such a system can reach 400 F/cm³ and by itself it becomes an electrical battery with an energy of about 200 kJ/l. When such a storage device is discharged, liquid is expelled from the channels at a pressure, which allows it to be used as a hydromotor without a moving mechanical elements (a capillary electric motor). A power of 1 kW/l can be achieved even with a capillary diameter of 1000 Å and a cycling frequency of 1 Hz. Such motors have essentially already been achieved in experimental devices, but with negligible power.

When a high-energy surface is formed, either by forcing liquid into channels or by removing an interphase potential difference or including a metal-dielectric transition through a temperature or pressure change, there is a change in the system entropy and absorption or release of heat. This effect may serve as a working principle for unconventional refrigeration cycles. Now we have a new working medium with the equation $PV = S(\delta_o - \delta_p P - \delta_t T - qE)$.

High energy of metal-dielectric interaction (Fig. 2) may effectively alter the properties of the thin metal and dielectric (semiconductor) layers in vicinity of the contact. It may be of importance for the electronic devices in micro-region.

Interphase interaction is very important for the systems with highly dispersed components. Using the zeolites and other porous matrices one can create a three-dimensional systems of microparticles (clusters) — a new type of solid bodies — cluster crystals.¹⁶⁾ If we shall

regard a cluster as a large atom-like particle with compressed energy level scale one can imagine the “cluster Periodic Table” the last being more various than the “atom Periodic Table” (in contrast to the case when the electrons changed by muons and all atoms become very small). This is a base for the possible cluster crystals diversity.

Cluster crystals are very sensitive for the external influences being very narrow energy gap systems. An as example may be mentioned the NaXTe₁₆ and NaXTe₂₃ cluster lattices with N and S-shaped voltage-current characteristics for electric field about 10³ V/cm.¹⁷⁾ NaAHg₁₃-system with magnetic phase transition under the magnetic field about 10⁴ G.¹⁸⁾ Potassium clusters incorporated into the zeolite LTA cavities are shows ferromagnetism.¹⁹⁾ Three-dimensional K₃C₆₀ cluster lattices are revealed superconducting behavior.²⁰⁾

Cluster crystals in zeolites matrices and cluster systems based on the carbon structures are resembled. In both cases the Mott-transition problem is arise also (interaction across the interphase layer).

The study of capillary effects in systems with extremely high dispersion is evidently of both scientific and practical interest for problems of chemical technology, electronics, energetics, and environmental engineering.

References

- 1) Ono, S., and Kondo, S., *Molecular Theory of Surface Tension in Liquids*, Springer-Verlag, Berlin, 1960.
- 2) Rowlinson, J. S., Widom, B., *Molecular Theory of Capillarity*, NY-London, Oxford University, 1982.
- 3) De Gennes, P. G., *Rev. Mod. Phys.*, 57, 827 (1985).
- 4) Bogomolov, V. N., *Fiz. Tverd. Tela.*, 5, 2011 (1963) [*Sov. Phys. Sol. St.*, 5, 1468 (1964)], 13, 815 (1971) [13, 672 (1971)], 14, 1228 (1972) [14, 1048 (1972)].
- 5) Breck, D. W., *Zeolite Molecular Sieves*, Wiley, N.Y., 1974.
- 6) Bogomolov, V. N., *Zh. Tekh. Fiz.*, 62, 152 (1992) [*Sov. Phys. Tech. Phys.*, 37, 79 (1992)].
- 7) Waber, J. T., Cromer, D. T., *J. Chem. Phys.*, 42, 4116 (1965).
- 8) Bucher, J. P., Buttet, J., Van der Klink, J. J., *Surface Science*, 214, 347 (1989).

- 9) Girifalco, L. A., Good, P., *J. Phys. Chem.*, 61, 904 (1957), 64, 561 (1960).
- 10) Saito, K., *Chemistry and Periodic Table*, Iwanami Shoten Publ., 1980.
- 11) Adamson, A. W., *Physical Chemistry of Surfaces*, Wiley, N.Y., 1976.
- 12) Meyer, K., *Physikalisch-Chemische Kristallographie*, VEB, Leipzig, 1968.
- 13) Yang, Ju-Xing, Koplík, J., Banavar, J. R., *Phys. Rev. Lett.*, 67, 3539 (1991).
- 14) Tauster, S. J., et al., *J. Am. Chem. Soc.*, 100, 170 (1978).
- 15) Bogomolov, V. N., *Excimer Interaction at the Condensation, Adsorption and Catalysis*, FTI Preprint No. 1536 (in Russian), A. F. Ioffe Phys. Tech. Inst., Leningrad, 1991.
- 16) Bogomolov, V. N., *Usp. Fiz. Nauk.*, 124, 171 (1978) [*Sov. Phys. Usp.*, 21, 77 (1978)].
- 17) Bogomolov, V. N., Zadorozhnyi, A. I., Pavlova, T. M., Petranovsky, V. P., Podchalusin, V. P., Cholkin, A. V., *Pisma ZETF*, 31, 406 (1980) [*JETP Lett.*, 31, 378 (1980)].
- 18) Bogomolov, V. N., Zadorozhnyi, A. I., Panina, L. K., *Physica*, 107B, 89 (1981).
- 19) Nozue, Y., Kodaira, T., Goto, T., *Phys. Rev. Lett.*, 68, 3789 (1992).
- 20) Hebard, A. F., *Phys. Today*, 156, 26 (1992).